Chelonian Conservation and Biology, 2022, 21(1): 122–12 doi:10.2744/CCB-1517.1 © 2022 Chelonian Research Foundation

Echoanatomical Features of the Major Cervical Blood Vessels of the Juvenile Green Sea Turtle (*Chelonia mydas*)

André Augusto Justo^{1,*}, Gustavo Henrique Pereira Dutra^{2,3}, Angélica Alfonso⁴, Gabriel Oliveira Silva², Fabio Celidonio Pogliani⁵, Adriano Bonfim Carregaro³, and Silvia Renata Gaido Cortopassi¹

*Corresponding author

ABSTRACT. – Although ultrasonographic examination of the blood vessels of sea turtles has been a helpful tool in the clinical setting, there is a paucity of data on the normal cervical echoanatomy of green turtles (*Chelonia mydas*); such information could be valuable for conservation-focused efforts at rehabilitation facilities. We studied the echoanatomical features of the major blood vessels of the neck of juvenile green turtles by gross dissection of 5 deceased turtles and by ultrasonographic examination of 11 healthy animals. The external jugular and the vertebral veins were superficial (< 1.5 cm) and presented an echogenic and turbulent pattern of blood flow in B-mode examination; carotid arteries lied deeply within the neck (> 1.5 cm) and exhibited a laminar blood flow characterized by a parabolic velocity profile as determined by Doppler sonography.

KEY WORDS. - anatomy; blood flow; Chelonia mydas; echocardiography; green sea turtle; ultrasonography

The green turtle (Chelonia mydas) is a sea turtle species classified as endangered on a global scale according to the International Union for Conservation of Nature (Seminoff 2004). In Brazil, it is the most common sea turtle species inhabiting the Brazilian coast, where important feeding grounds are found for nutritional support during growth (Fernandes et al. 2017). However, shallow coastal waters pose a constant threat to the foraging juveniles due to human activities, which include artisanal fisheries, marine traffic, ports, and pollution (Fuentes et al. 2020). Turtles that are injured by these activities are often presented to rehabilitation centers for medical management. Moreover, in highly degraded neritic habitats, fibropapillomatosis is a prevalent disease particularly affecting green turtles (Dos Santos et al. 2010) and is deemed a health concern to juvenile individuals in rehabilitation centers (Page-Karjian et al. 2014; Rossi et al. 2019). At these facilities, in-depth clinical and laboratory evaluations are essential for assessing the progress of rehabilitation and the efficacy of medical management.

Cardiovascular ultrasonography is a useful diagnostic tool in chelonians, providing rapid, simple, and noninvasive imaging of the heart and its vessels (Penninck et al. 1991). Transplastral ultrasonography was effective for assessing the hemodynamics of major arteries (e.g., left and right aortic arches and pulmonary artery) in debilitated green turtles (March et al. 2021). The appearance and flow patterns of peripheral blood vessels (e.g., internal iliac artery, epigastric artery, and renal vein) were also assessed by ultrasonography in loggerhead sea turtles (*Caretta caretta*) (Valente et al. 2007, 2008).

Cervical ultrasonography could provide valuable contributions for the clinical setting since major blood vessels run along the neck of sea turtles. The jugular vein is the most commonly used venipuncture site for blood collection in sea turtles (Owens and Ruiz 1980; Perpiñán 2017), although successful venipuncture at this site relies on "blind" puncture and personal expertise given the lack of easily identifiable external anatomical landmarks. In this context, cervical echographic imaging is sometimes used to assist with vessel localization for blood sampling and intravenous drug delivery (Wyneken et al. 2006; Dutra et al. 2014). Vascular catheterization may also benefit from ultrasound-guided techniques, which could be of consid-

¹Department of Surgery, School of Veterinary Medicine and Animal Science, University of São Paulo (USP), São Paulo, São Paulo 05508-270, Brazil [andre.justo@usp.br; silcorto@usp.br];

²Veterinary Unit of the Santos Aquarium, Santos Aquarium, Santos, São Paulo 11030-500, Brazil [gustavodutra@usp.br; gabrieldh.silva@outlook.com];

³Department of Veterinary Medicine, School of Animal Science and Food Engineering, University of São Paulo (USP), Pirassununga, São Paulo 13635-900, Brazil [carregaro@usp.br];

⁴Department of Veterinary Clinic, School of Veterinary Medicine and Animal Science, São Paulo State University (UNESP), Botucatu, São Paulo 18618-681, Brazil [alfonso_angelica@ymail.com];

⁵Department of Internal Medicine, School of Veterinary Medicine and Animal Science, University of São Paulo (USP), São Paulo, São Paulo (05508-270, Brazil [fabiocp@usp.br]

erable help in severely debilitated turtles that require fluid therapy (Di Bello et al. 2010). Ultimately, echographic assessment of peripheral arterial hemodynamics analysis may improve the diagnostic evaluation of cardiovascular status and aid resuscitation procedures in sea turtles (Stabenau and Moon 2001; Valente et al. 2008).

However, there is a gap in the literature regarding the ultrasonographic technique and normal echoanatomical features of the cervical blood vessels across sea turtle species (Wyneken 2001; Valente et al. 2008). In the present study, we provide gross anatomical data and describe normal echographic images of the major cervical blood vessels in the juvenile green turtle.

METHODS

Sixteen juvenile green turtles of unknown sex were enrolled in this study. Animals weighed 18.1 ± 5.4 kg (11.1-26.2) and had a straight carapace length of 47.3 ± 5.3 cm (35-55) (mean \pm SD [range]). All turtles were caught by trained stranding personnel along the southern coast of São Paulo in Brazil (lat $23^{\circ}59'-24^{\circ}19'$ S, long $46^{\circ}18'-46^{\circ}59'$ W) and were admitted to the rehabilitation facilities of the Santos Aquarium for fibropapillomatosis treatment (n = 14) or because of boat strike injuries (n = 2).

Of the 16 individuals received, 5 died during rehabilitation. The deceased turtles were used for macroscopic description of the cervical vasculature and to define the most adequate sites for ultrasound scanning. The cause of death did not interfere with the aims of the current research. Dissections were performed in unfixed fresh carcasses with the head slightly ventroflexed over the edge of a table and followed the guidelines and terminology available for sea turtles (Wyneken 2001). Briefly, the skin and subcutaneous tissues of the neck were removed, followed by dissection of the superficial cervical muscles and major cervical veins. To locate the carotid arteries, the plastron was detached and the heart exposed. The carotids were identified as they emerged from the right systemic aortic arch and then were traced toward the cervical region.

The ultrasonographic study was carried out in the remaining 11 turtles prior to release, all of which were considered to be healthy on the basis of a physical examination and results of a blood cell count and biochemistry panel (Bolten and Bjorndal 1992). Animals were manually restrained in ventral recumbency above a foamed mattress, with the head hanging free off its edge. Ultrasound imaging was performed by a portable ultrasound device (Sonosite M-Turbo, Fujifilm Sonosite) equipped with a multifrequency (6–13 MHz) linear electronic transducer. Coupling gel (Aquasonic Parker) was applied on the surface of the transducer, which was placed mainly perpendicularly to the cervical skin surface (cervical acoustic window).

Real-time, 2-dimensional scanning was used to locate the blood vessels and to assess their morphology, including wall echogenicity, intraluminal content, and vessel diameter. At the vessel's widest diameter, the distance from the leading edge of the intima-lumen interface of the near wall to the leading edge of the lumen-intima interface of the far wall was measured and reported as blood vessel diameter. Color and pulsed wave Doppler sonography were used to determine the direction, peak systolic velocity, and waveform pattern of the carotid blood flow. Doppler tracings were registered when the angle between the long axis of the blood flow and that of the ultrasound beam was below 60°. Freeze trace and cineloop images were obtained during Doppler sonography scans, and the peak systolic velocity was averaged over 3 consecutive measurements.

Room temperature was maintained at 25°C during the exams. Each ultrasonographic session lasted approximately 20 min, and no chemical restraint was required. One experienced operator (A.A.) conducted all ultrasound examinations.

The software GraphPad Version 8 (GraphPad Software Inc) provided statistical analysis. Data symmetry was verified by the Shapiro-Wilk test, and a paired t-test was used to compare peak systolic velocity and/or diameter in paired vessels (left and right sides). The statistical significance was set at $p \leq 0.05$. Descriptive statistics are reported as mean \pm SD (range).

RESULTS

During dissection, the biventer and the transverse cervical muscles were prominent immediately following subcutaneous connective tissue removal and provided adequate landmarks for subsequent identification of the cervical blood vessels. In a dorsal view, the biventer muscle was the dorsalmost structure observed, running parallel with the longitudinal axis of the neck and resting on the dorsolateral aspect of the cervical vertebrae arch (Fig. 1). A single vertebral vein was noted between the left and right biventer cervical muscles (Fig. 1). It occupied a central position on the dorsal neck, emerging from the skull caudal to the supraoccipital crest. Caudally, at twothirds the length of the neck, the vertebral vein branched into the 2 transverse cervical veins, which extended laterally to meet the external jugular veins (Fig. 1). The transverse cervical muscle extended laterally in the neck and followed an oblique path from the direction of the first marginal scute, ending lateral of the hyoid process (Figs. 1 and 2).

The external jugular veins were the largest cervical blood vessels observed in the juvenile green turtle and were positioned in a dorsolateral and superficial position in the neck. They ran adjacent to the ventrolateral aspect of the biventer cervical muscle and medial to the transverse cervical muscle, extending from the base of the skull into the subcarapacial space (Fig. 2). The transverse cervical



Figure 1. Anatomical view of the dorsal aspect of the neck of a juvenile green turtle following removal of the subcutaneous connective tissue. Key: 1 = transverse cervical muscle; 2 = biventer cervical muscle; 3 = vertebral vein; 4 = transverse cervical vein; 5 = external jugular vein; 6 = supraoccipital crest; 7 = first marginal scute; 8 = nuchal scute. Photo by A. Justo.



Figure 2. Anatomical view of the dorsolateral aspect of the neck of a juvenile green turtle following removal of the subcutaneous connective tissue. The carotids were pulled laterally to become visible. Key: 1 = transverse cervical muscle; 2 = biventer cervical muscle; 3 = vertebral vein; 4 = transverse cervical vein; 5 = external jugular vein; 6 = supraoccipital crest; 7 = first marginal scute; 8 = hyoid process; 9 = internal jugular vein; 10 = carotid artery. Photo by A. Justo.



Figure 3. Dorsal cervical view of a debilitated juvenile green turtle where the suspensory muscles of the neck are used as landmarks to locate the superficial veins (dashed lines). The transverse cervical muscles are indicated by filled arrowheads and the biventer cervical muscles by empty arrowheads. Photo by A. Justo.

veins were the only cervical veins connected to the jugulars. The internal jugular veins were smaller than the external veins and were found more deeply in the neck in close association with the carotid arteries (Fig. 2). The superficial suspensory muscles of the neck were readily visualized in debilitated green turtles, which provided guidance to locate the external jugular vein, the vertebral vein, and the carotid artery (Figs. 3 and 4). The carotid arteries arose from the brachiocephalic trunk of the right aortic arch (Fig. 5). At the neck, they resided deep to cervical ventral muscles; thus, for didactic purposes, the carotids were pulled laterally to become visible (Fig. 2).

Sonographically, the vertebral vein was visible in a longitudinal projection as the transducer was placed on the dorsal sagittal midline of the cervical skin (in the 12:00 position), with the marker oriented toward the carapace (Fig. 6A). The echoanatomy of the vertebral vein consisted of a superficial (0.5–1 cm deep) tubular structure, with walls that easily collapsed on application of light pressure by the transducer (Fig. 6B). Mean \pm SD vertebral vein diameter was 0.70 \pm 0.19 cm (range, 0.5–0.98 cm). Clockwise rotation of the ultrasound probe at the middorsal cervical region allowed for a transverse scan of the vertebral vein (Fig. 7A). In this projection, the

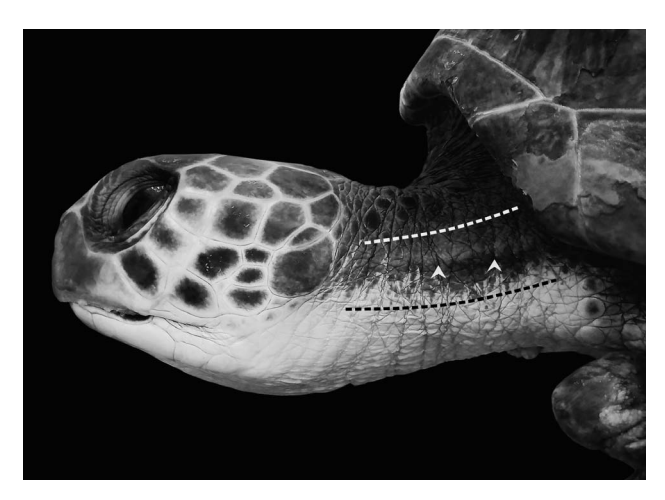


Figure 4. Lateral cervical view of a debilitated juvenile green turtle where the transverse cervical muscle (filled arrowheads) is used as a landmark to locate the external jugular vein (white dashed line) and the carotid artery (black dashed line). Photo by A. Justo.

external jugular veins were also transversely imaged lying at each side of the vertebral vein (Fig. 7B). The echogenic borders of the cervical vertebrae produced a strong reflection of the osseous tissue as seen by acoustic



Figure 5. Anatomical view of the ventral aspect of the heart and its major arteries from a juvenile green turtle following removal of the pericardial sac. Key: 1 = ventricle; 2 = right atrium; 3 = left atrium; 4 = pulmonary artery; 5 = left aorta; 6 = brachiocephalic trunk; 7 = right aorta; 8 = right subclavian artery; 9 = carotid arteries. The left subclavian artery is not dissected free of its connective tissue. Photo by A. Justo.

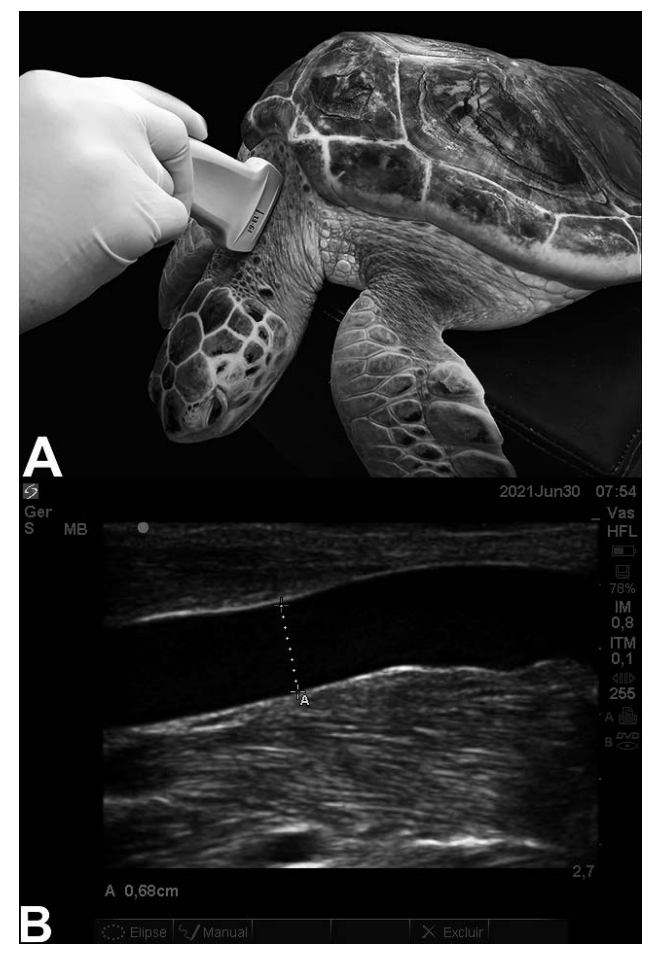


Figure 6. Probe-positioning in the sagittal plane with the marker oriented toward the carapace (A). Two-dimensional longitudinal scan of the vertebral vein (B). Cursors measure the diameter. Photo by A. Justo.

shadowing (Fig. 7C). Visualization of the transverse cervical veins was inconsistent.

Consistent and repeatable sonographic images of the external jugular veins were best achieved through a longitudinal scan. The transducer was placed in a parasagittal plane between the biventer and the transverse cervical muscles at approximately 11:00 and 1:00 for the right and the left sides, respectively (Fig. 8A). At this location, the external jugular vein appeared as a large vessel (Fig. 8B). Jugular diameter did not differ between the right and left sides (p = 0.089; overall mean \pm SD of 1.22 ± 0.36 cm [range, 0.85-1.72 cm]). In all animals, B-mode flow imaging of the external jugular and vertebral veins revealed turbulent, amorphous, and echogenic particles, similar to a light gray haze (Figs. 6B and 8B). The internal jugular veins could not be detected by ultrasonography.

Sonographically, carotids were imaged at the midline of the lateral of the neck (in the 9:00 and 3:00 positions for the right and left sides, respectively) with a 50°-60° angle between the long axis of the neck and the transducer surface. The marker was oriented caudally (Fig. 9A). Ultrasonographic identification was based on their location



Figure 7. Probe-positioning in the transverse plane at the mid dorsal cervical skin surface (A). Two-dimensional transverse scan of the vertebral and external jugular veins (B, C). Key: 1 =external jugular vein; 2 =vertebral vein; 3 =dorsal arch of the cervical vertebrae; 4 =spinal cord; 5 =vertebral body; 6 =acoustic shadowing. Photo by A. Justo.

(1.5–2.5 cm deep) and cranial direction of the pulsatile blood flow (Fig. 9B–C). Vessel walls appeared as parallel hyperechoic lines, and luminal content was homogeneously hypoechogenic. No differences were found in the diameter (p = 0.534; overall mean \pm SD of 0.29 \pm 0.06 cm [range, 0.21–0.41 cm]) and in the peak systolic velocity (p = 0.812; overall mean \pm SD of 14.26 \pm 2.83



Figure 8. Probe-positioning in the parasagittal plane at the dorsolateral cervical skin surface, with the marker oriented toward the carapace (A). Two-dimensional longitudinal scan of the external jugular vein (B). Cursors measure the diameter. Photo by A. Justo.

cm/sec [range, 10.80–19.43 cm/sec]) between the right and the left carotid arteries. The carotids had a laminar flow consisting of a parabolic velocity profile, as noted on pulsed wave Doppler sonography. This was indicated by a broad systolic peak without spectral window and a gradually decreasing velocity in diastole (Fig. 9D).

DISCUSSION

The branching pattern of the external jugular vein of green turtles documented in this study is in line with earlier reports, where few jugular branches were also observed in this species (Wyneken 2001). The carotid arteries emerged from the brachiocephalic trunk of the right aortic arch and not from the subclavian arteries, as has been recorded in other sea turtle species (Wyneken 2001).

The jugular vein is the site traditionally used for percutaneous catheter placement, blood sampling, and intravenous drug delivery in sea turtles (Wyneken et al. 2006; Dutra et al. 2014). However, unlike in tortoises (Mans 2008), direct visualization of the jugulars is not

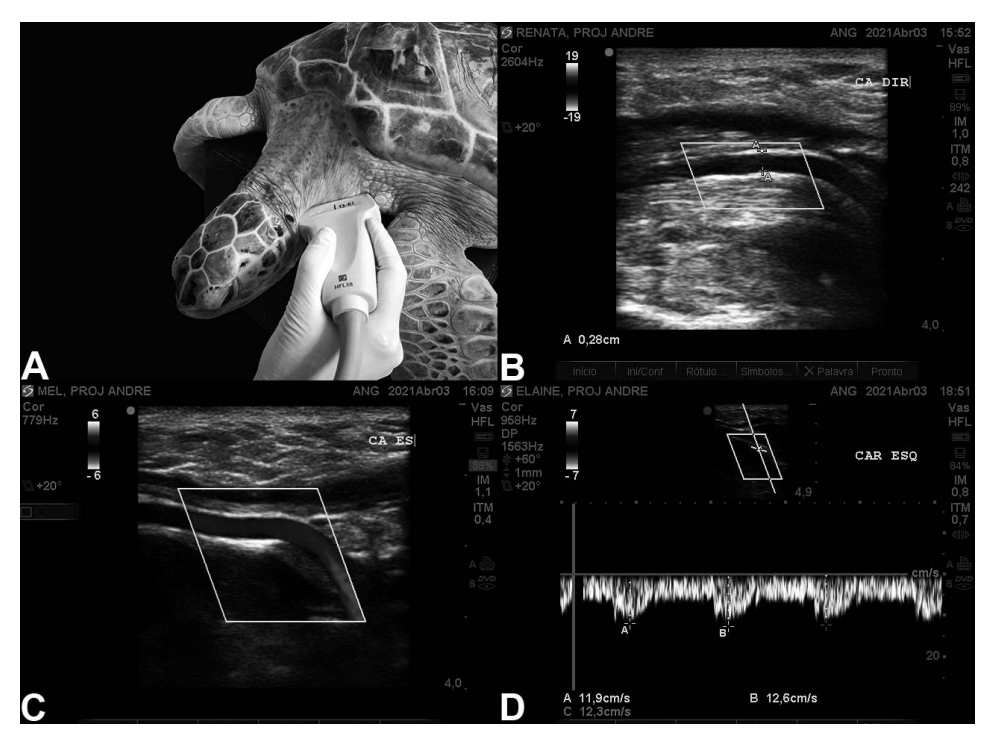


Figure 9. Probe-positioning in the frontal plane, with the transducer oriented parallel to the plastron in a 50° – 60° angle to the long axis of the neck (A). Two-dimensional longitudinal scan of the carotid artery (B). Cursors measure the diameter. Color flow (C) and pulsed wave Doppler tracing (D) of the carotid artery. Photo by A. Justo.

possible in sea turtles. Based on the current echoanatomical findings, ultrasonography represents a feasible option for visualizing the superficial veins of green turtles and, therefore, may be an alternative to the surgical approaches often required to locate and catheterize the jugular vein (Briscoe and Syring 2004; Wyneken et al. 2006). Severely dehydrated chelonians may pose extra challenges to jugular access due to poor peripheral perfusion (Briscoe and Syring 2004), which further supports the use of ultrasonography in the clinical setting. Moreover, ultrasound-guided jugular puncture circumvents the repeated neck punctures often performed for blood sampling in "blind" techniques (Owens and Ruiz 1980) and hence should minimize the animals' stress.

The vertebral vein proved to be easily imaged. Access to the vertebral vein could be especially useful when access to the jugular vein is not possible, as in fibropapillomatosis-afflicted individuals presenting multiple tumors on the neck, which accounts for the third most affected part of the body in green turtles (Rossi et al. 2016).

The most distinctive feature of the external jugular and vertebral veins of green turtles was the echogenic and turbulent blood flow. This sonographic pattern is termed "spontaneous echographic contrast" and derives from the backscattering of ultrasound produced by red cell aggregates (Reeder et al. 1994). Although erythrocyte aggregation-induced echogenicity is multifactorial (e.g., increased temperature, hematocrit and plasmatic proteins, or low-flow states) (Sigel et al. 1982, 1983), this phenomenon has been used mainly as a marker for blood

stasis and thromboembolic disorders in mammalian species (Black 2000; Peck et al. 2016). In sea turtles, resting blood pressure and heart rate values are low in comparison to mammals (Moon and Stabenau 1996), which may contribute to the development of a more sluggish blood flow. In addition to being observed in all of the turtles included in the present study, spontaneous echo contrasts have also been documented for the intracardiac flow of green turtles (March et al. 2021) and for the dorsal cervical sinuses of loggerheads (Valente et al. 2007), thereby suggesting to be a normal finding in sea turtles.

Whereas previous studies have questioned the ease of carotid imaging in sea turtles given its deep location within the neck (Valente et al. 2008), both carotids were easily assessed in green turtles. The velocity profile of the carotid arteries of green turtles was remarkable compared with that of mammals. In this study, systolic peaks had a broad velocity distribution (i.e., parabolic pattern), which is opposite to the narrow velocity distribution and sharp systolic peak (i.e., plug pattern) documented in mammals (Lee et al. 2004; Jung et al. 2010; Svicero et al. 2013). Such a velocity profile had also been observed for the right aortic arch of loggerheads (Valente et al. 2008) and is consistent with organs having a continuous blood demand, which is met by a continuing high flow during diastole (Szatmári et al. 2001). Our sonographic findings corroborate early studies demonstrating that the circulation to the head never ceases in sea turtles (Hochscheid et al. 2002). This represents an adaptation to diving common to aquatic air-breathing animals in that blood is optimized for the

functioning of vital organs during apnea (e.g., brain) (Handrich et al. 1997).

In sea turtles, as in many species, the carotids are responsible for supplying blood to the head, including the brain (Wyneken 2001). For this reason, carotid imaging could provide objective data to monitor the improvement or decline of systemic perfusion in response to cardiopulmonary resuscitation attempts, helping to discern a still-living turtle from a recently deceased turtle (Wyneken et al. 2006). This is supported by studies in mammals in that the increased peak systolic velocity of the carotid artery following resuscitation from cardiac arrest was used as a reliable predictor of outcome and brain damage (Fukushima et al. 2000). Similarly, increased blood flow in the pulmonary artery and aorta was recently described in Australian green turtles as they recovered from illness (March et al. 2021). Therefore, although further study is needed, it is possible that sonographic evaluation of carotid hemodynamic data could provide prognostic information for moribund sea turtles, in which weak cardiac contractility is often the only evidence that they are still alive (Spielvogel et al. 2017).

Results of the current study will provide valuable information for the clinical management of green turtles, including the collection of blood samples, catheterization, and the recognition of abnormal vascular states. In addition, the documented echoanatomical parameters can be used as reference for further studies on other sea turtle species.

ACKNOWLEDGMENTS

This study was funded by grant no. 2020/02439-3, São Paulo Research Foundation (FAPESP), and by the "Coordenação de Aperfeiçoamento de Pessoal de Nível Superior" (CAPES), Finance Code 001. This work was approved by the Institutional Animal Care and Use Committee of the School of Veterinary Medicine and Animal Science, University of São Paulo (USP) (protocol no. 1884030220), and by the Brazilian Biodiversity Information and Authorization System (SISBIO no. 74546-1). We would also like to thank the staff of the Santos Aquarium for logistical support during the study.

COPYRIGHT LICENSE

This is an open access article published under the Creative Commons CC-BY-NC-SA license (https://creativecommons.org/licenses/by-nc-sa/4.0/), which means the article may be reused with proper attribution for non-commercial use. Any remix or transformed version of the content must be distributed under the same license as the original.

LITERATURE CITED

Black, I.W. 2000. Spontaneous echo contrast: where there's smoke there's fire. Echocardiography 17(4):373–382.

- Bolten, A.B. and Bjorndal, A. 1992. Blood profiles for a wild population of green turtles (*Chelonia mydas*) in the southern Bahamas: size-specific and sex-specific relationships. Journal of Wildlife Diseases 28:407–413.
- Briscoe, J.A. and Syring, R. 2004. Techniques for emergency airway and vascular access in special species. Seminars in Avian and Exotic Pet Medicine 13(3):118–131.
- DI BELLO, A., VALASTRO, C., FREGGI, D., SAPONARO, V., AND GRIMALDI, D. 2010. Ultrasound-guided vascular catheterization in loggerhead sea turtles (*Caretta caretta*). Journal of Zoo and Wildlife Medicine 41:516–518.
- Dos Santos, R.G., Martins, A.S., Torezani, E., Baptistotte, C., Da Nóbrega Farias, J., Horta, P.A., Work, T.M., and Balazs, G.H. 2010. Relationship between fibropapillomatosis and environmental quality: a case study with *Chelonia mydas* off Brazil. Diseases of Aquatic Organisms 89(1):87–95.
- Dutra, G.H.P., Futema, F., Santos, F.A.M., and Nascimento, C.L. 2014. Intravascular access in *Chelonia mydas* and *Dermochelys coriacea* using the Seldinger technique ultrasound-guided. Journal of Life Sciences 8(5):385–393.
- Fernandes, A., Bondioli, A.C.V., Solé, M., and Schiavetti, A. 2017. Seasonal variation in the behavior of sea turtles at a Brazilian foraging area. Chelonian Conservation and Biology 16:93–102.
- FUENTES, M.M.P.B., WILDERMANN, N., GANDRA, T.B.R., AND DOMIT, C. 2020. Cumulative threats to juvenile green turtles in the coastal waters of southern and southeastern Brazil. Biodiversity and Conservation 29(6):1783–1803.
- Fukushima, U., Sasaki, S., Okano, S., Oyamada, T., Yoshikawa, T., Hagio, M., and Takase, K. 2000. Non-invasive diagnosis of ischemic brain damage after cardiopulmonary resuscitation in dogs by using transcranial Doppler ultrasonography. Veterinary Radiology and Ultrasound 41(2):172–177.
- Handrich, Y., Bevan, R.M., Charrassin, J., Butler, P.J., Puetz, K., Woakes, A.J., Lage, J., and Maho, Y.L. 1997. Hypothermia in foraging king penguins. Nature 388:64–67.
- HOCHSCHEID, S., BENTIVEGNA, F., AND SPEAKMAN, J.R. 2002. Regional blood flow in sea turtles: implications for heat exchange in an aquatic ectotherm. Physiological and Biochemical Zoology 75(1):66–79.
- JUNG, J., CHANG, J., OH, S., AND CHOI, M. 2010. Spectral Doppler ultrasound in the major arteries of normal conscious immature micropigs. Journal of Veterinary Science 11(2):155–159.
- Lee, K., Choi, M., Yoon, J., and Jung, J. 2004. Spectral waveform analysis of major arteries in conscious dogs by doppler ultrasonography. Veterinary Radiology and Ultrasound 45(2):166–171.
- Mans, C. 2008. Venipuncture techniques in chelonian species. Lab Animal 37(7):303–304.
- MARCH, D.T., MARSHALL, K., SWAN, G., GERLACH, T., SMITH, H., BLYDE, D., ARIEL, E., CHRISTIDIS, L., AND KELAHER, B.P. 2021. The use of echocardiography as a health assessment tool in green sea turtles (*Chelonia mydas*). Australian Veterinary Journal 99(1–2):46–54.
- Moon, P.F. and Stabenau, E.K. 1996. Anesthetic and postanesthetic management of sea turtles. Journal of the American Veterinary Medical Association 208(5):720–726.
- Owens, D.W. AND Ruiz, G.J. 1980. New methods of obtaining blood and cerebrospinal fluid from marine turtles. Herpetologica 36(1):17–20.
- PAGE-KARJIAN, A., NORTON, T.M., KRIMER, P., GRONER, M., NELSON, S.E., AND GOTTDENKER, N.L. 2014. Factors influencing survivorship of rehabilitating green sea turtles (*Chelonia mydas*) with fibropapillomatosis. Journal of Zoo and Wildlife Medicine 45(3):507–519.

- Peck, C.M., Nielsen, L.K., Quinn, R.L., Laste, N.J., and Price, L.L. 2016. Retrospective evaluation of the incidence and prognostic significance of spontaneous echocardiographic contrast in relation to cardiac disease and congestive heart failure in cats: 725 cases (2006–2011). Journal of Veterinary Emergency and Critical Care 26(5):704–712.
- Penninck, D.G., Stewart, J.S., Paul-Murphy, J., and Pion, P. 1991. Ultrasonography of the California desert tortoise (*Xerobates agassizi*): anatomy and application. Veterinary Radiology 32(3):112–116.
- Perpiñán, D. 2017. Chelonian haematology 1. Collection and handling of samples. In Practice 39(5):194–202.
- REEDER, G.S., CHARLESWORTH, J.E., AND MOORE, S.B. 1994. Cause of spontaneous echographic contrast as assessed by scanning electron microscopy. Journal of the American Society of Echocardiography 7(2):169–173.
- Rossi, S., Sánchez-Sarmiento, A.M., Dos Santos, R.G., Zamana, R.R., Prioste, F.E.S., Gattamorta, M.A., Ochoa, P.F.C., Grisi-Filho, J.H.H., and Matushima, E.R. 2019. Monitoring green sea turtles in Brazilian feeding areas: relating body condition index to fibropapillomatosis prevalence. Journal of the Marine Biological Association of the United Kingdom 99(8):1879–1887.
- Rossi, S., Sánchez-Sarmiento, A.M., Vanstreels, R.E.T., Dos Santos, R.G., Prioste, F.E.S., Gattamorta, M.A., Grisi-Filho, J.H.H., and Matushima, E.R. 2016. Challenges in evaluating the severity of fibropapillomatosis: a proposal for objective index and score system for green sea turtles (*Chelonia mydas*) in Brazil. PLoS One 11(12):1–11.
- Seminoff, J.A. 2004. Chelonia mydas. The IUCN Red List of Threatened Species. 2004:e.T4615A11037468.
- SIGEL, B., COELHO, J.C.U., SCHADE, S.G., JUSTIN, J., AND SPIGOS, D.G. 1982. Effect of plasma proteins and temperature on echogenicity of blood. Investigative Radiology 17(1):29–33.
- SIGEL, B., MACHI, J., BEITLER, J.C., AND JUSTIN, J.R. 1983. Red cell aggregation as a cause of blood-flow echogenicity. Radiology 148(3):799–802.

- SPIELVOGEL, C.F., KING, L., CAVIN, J.M., TLUSTY, M., SILVERSTEIN, D.C., CERESIA, M.L., AND INNIS, C.J. 2017. Use of positive pressure ventilation in cold-stunned sea turtles: 29 cases (2008–2014). Journal of Herpetological Medicine and Surgery 27(1–2):48–57.
- STABENAU, E.K. AND MOON, P.F. 2001. Resuscitation of sea turtles. Marine Turtle Newsletter 62:3–5.
- SVICERO, D.J., DOICHE, D.P., MAMPRIM, M.J., HECKLER, M.C.T, AND AMORIM, R.M. 2013. Ultrasound evaluation of common carotid artery blood flow in the Labrador retriever. BMC Veterinary Research 9:1–5.
- SZATMÁRI, V., SÓTONYI, P., AND VÖRÖS, K. 2001. Normal duplex doppler waveforms of major abdominal blood vessels in dogs: a review. Veterinary Radiology and Ultrasound 42(2): 97–107.
- VALENTE, A.L., PARGA, M.L., ESPADA, Y., LAVIN, S., ALEGRE, F., MARCO, I., AND CUENCA, R. 2007. Ultrasonographic imaging of loggerhead sea turtles (*Caretta caretta*). Veterinary Record 161(7):226–232.
- Valente, A.L., Parga, M.L., Espada, Y., Lavin, S., Alegre, F., Marco, I., and Cuenca, R. 2008. Evaluation of Doppler ultrasonography for the measurement of blood flow in young loggerhead sea turtles (*Caretta caretta*). Veterinary Journal 176(3):385–392.
- WYNEKEN, J. 2001. The Anatomy of Sea Turtles. US Department of Commerce NOAA Tech. Memor. NMFS-SEFSC 470, pp. 1–172.
- Wyneken, J., Mader, D.R., and Weber, E.S. 2006. Medical care of sea turtles. In: Mader, D. (Ed.). Reptile Medicine and Surgery. Second edition. St. Lous, MO: Saunders, pp. 972–1007.

Received: 9 September 2021

Revised and Accepted: 17 February 2022

Published Online: 13 June 2022 Handling Editor: Jeffrey A. Seminoff